THE EFFECT OF STRAIN RATE ON THE J-INTEGRAL

S. Kodama*, H. Misawa*, M. Hasegawa** and H. Nakayama***

*Faculty of Technology, Tokyo Metropolitan Univ., Fukasawa, Setagaya-ku, Tokyo, 158, Japan.
**Technological Univ. of Nagaoka, Kamitomioka, Nagaoka City, Niigata-ken, 949-54, Japan.
***Hino Motor Co., Hino City, Tokyo, 191, Japan.

ABSTRACT

The toughness of Boron steel (SAE 10B35), quenched and tempered at the three tempering temperatures has been studied. Fracture toughness tests were carried out on 1/2 inch thickness compact tension specimens at four crosshead speeds: 0.1; 1.0; 10.0; and 100.0 mm/min. J_{IC} was determined from the onset of slow crack growth, which was detected by the AC electrical potential method. The experimental results show that J_{IC} values decrease with increasing strain rate, and can be correlated with the fracture toughness at lower temperature.

KEYWORDS

J_{IC}; strain rate; AC electrical potential method; low temperature; yield strength.

INTRODUCTION

The effect of loading rate or strain rate on the yielding characteristics of metals has long been of interest, and has often been considered together with the effect of temperature. Since the development of linear elastic fracture mechanics, the effect of the rate of change in the stress intensity factor, $\dot{K}$, on the fracture toughness, K_{IC}, has been studied (Crosly, 1976; Knott, 1973), together with the effect of temperature (Kraft, 1963; Corten, 1967; Shabbits, 1970; Burns, 1973). However, little work has been done on the effect of loading rate in nonlinear elastic-plastic or fully plastic fracture mechanics, or on the critical J-integral, J_{IC}.

The purpose of this study is to show experimentally the effect of loading rate on J_{IC} values, and to discuss the relation to the effect of the low temperatures and yield strength.

EXPERIMENTAL PROCEDURE

Boron steel (SAE 10B35) was used for these experiments, since the ductility of this material can be widely changed by suitable heat treatments. The chemical composition of the 10B35 used is shown in Table 1. Half inch thickness compact tension specimens were employed, as shown in Fig. 1. The specimens were machined to size, a chevron-shaped saw cut made at the notch root, and a fatigue crack introduced by cyclic tensile fatigue loading. The heat treatment was performed after the machining, but prior to the fatigue cracking. Specimens were oil quenched from 850°C (30min.) and then tempered at either 200°C, 400°C or 600°C for 2 hours, followed by water quenching. The mechanical properties of the heat treated materials are shown in Table 2.

Fracture toughness tests were carried out on an Instron-type universal testing machine at four levels of crosshead speed: 0.1; 1.0; 10.0; and 100.0 mm/min. Tensile tests were also performed on 5mm thick tensile specimens, at the same crosshead speeds.

For the determination of J, the following equations, proposed by Merkle and Corten (1974), was used:

$$
\left.
\begin{aligned}
J &= \frac{\eta_A A + \eta_C C}{Bb} \\
\eta_A &= \frac{2(1+\alpha)}{1+\alpha^2} \\
\eta_C &= \frac{2\alpha(1-2\alpha-\alpha^2)}{(1+\alpha^2)^2} \\
\alpha &= \sqrt{(\tfrac{a}{c})^2+2(\tfrac{a}{c})+2} - (\tfrac{a}{c}+1)
\end{aligned}
\right\} \quad \text{---(1)}
$$

Where: A= area under the load-displacement curve,
B= specimen thickness,
b= ligament,
c= b/2,
a= crack length,
C= area A complementary area under the load-displacement curve.

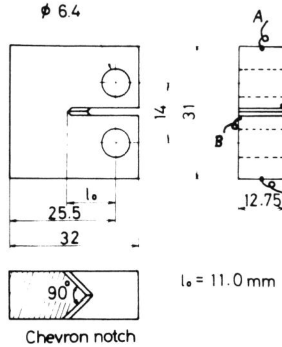

Fig. 1. Specimen geometry, showing AC potential drop lead positions.
A: AC current source
B: Output to p.d. amplifier.

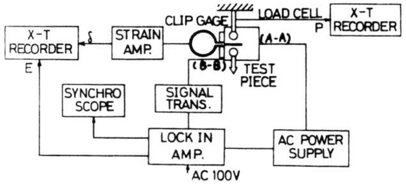

Fig. 2. J_{IC} test measuring system.

Table 1 Chemical composition of 10B35 (w.t. %)

C	Si	Mn	P	S	Cu	Ni	Cr	Al	Ti	B
0.36	0.26	0.83	0.017	0.010	0.010	0.020	0.140	0.020	0.024	0.0009

Table 2 Material mechanical properties

Tempering temp. of specimens	σ_{ys} kg/mm²	σ_B kg/mm²	σ_f kg/mm²	Elongation %	Reduction in area %	Vickers hardness
200°C	172.0	178.3	146.0	12.4	23.6	569
400°C	105.6	116.2	90.4	14.8	42.5	392
600°C	70.2	79.9	61.4	22.9	48.5	276

The J_{IC} criterion was determined from the onset of slow crack growth, as detected electrically. AC current was used instead of the conventional direct current, and the electrical potential across the notch was measured with a "lock-in amplifier" (phase sensitive detector amplifier). The positions of the electrical leads are shown in Fig. 1. The AC measuring system is shown in Fig. 2.

Following the fracture tests, the stretched zone width (SZW) was measured in the scanning electron microscope, so as to determine J_{IC} by another method. Besides the room temperature tests, further tensile and fracture toughness tests were carred out at low temperatures, at about 0.2 mm/min crosshead speed. In these fracture tests, the critical stress intensity factor K_{IC} or K_C was calculated according to ASTM E-399.

EXPERIMENTAL RESULTS

Tension test at room temperature and low temperatures

The variation of yield stress, σ_y, with strain rate and temperature is shown in Fig. 3 and Fig. 4 respectively. From these the effects the strain rate and temperature can be seen, the yield stress of the 400°C and 600°C tempered materials increasing with increasing strain rate, $\dot{\varepsilon}$, and decreasing temperature, T. The yield stress of the 200°C tempered material, however, is not affected by strain rate, and hardly affected by temperature.

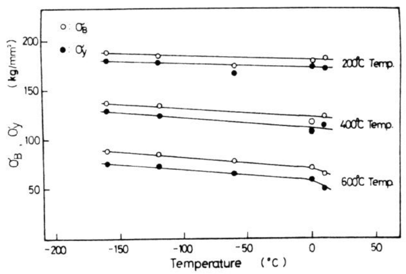

Fig. 3. Variation of yield stress with temperature.

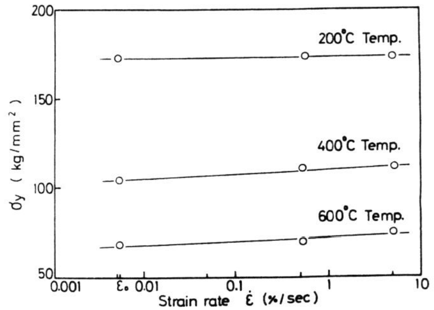

Fig. 4. Variation of yield stress with strain rate.

Room temperature fracture toughness tests

Typical room temperature load, clip gage displacement and potential drop curves for each of the tempering treatments are shown in Fig. 5, Fig. 6 and Fig. 7, respectively. The arrows on the potential drop curves indicate the onset of slow crack growth. The area A in equation (1) is determined up to this point on the load-displacement curve, and the resulting J value recorded as J_{IC} if it satisfied the following specimen size requirement:

$$B \text{ or } b \geq 25(J_{IC}/\sigma_y). \qquad \text{-----(2)}$$

The variation of J_{IC} with $\dot{\varepsilon}$ is shown in Fig. 8, where the crack tip strain rate $\dot{\varepsilon}$ is calculated from the equation

$$\dot{\varepsilon} = \dot{V}/2\rho, \qquad \text{-----(3)}$$

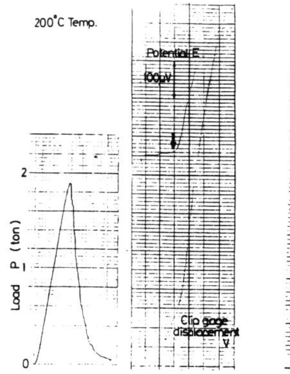

Fig. 5. Room temperature fracture toughness records for 200°C tempered material. 1mm/min crosshead speed.

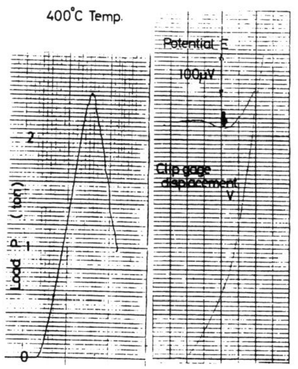

Fig. 6. Room temperature fracture tuoghness records for 400°C tempered material. 1mm/min crosshead speed.

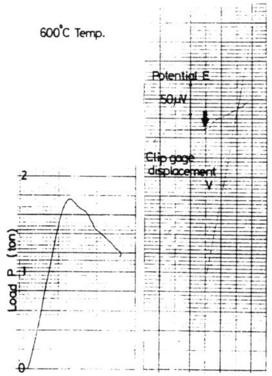

Fig. 7. Room temperature fracture toughness records for 600°C tempered material. 1mm/min crosshead speed.

$\dot{V}$ being the crack tip opening velocity as calculated from the clip gage displacement velocity, $\dot{\delta}$, and ρ is the equivalent crack tip radius. The value of ρ was here taken to be 0.05 mm for the three tempered materials, since the fracture toughness value measured in fatigue cracked specimens was equal to the fracture toughness in notched specimens with an 0.05 mm notch root radius (Knott, 1973).

All J_{IC} values satisfied the validity equation (2). The results show that J_{IC} values decreased with increasing strain rate $\dot{\varepsilon}$ in the 400°C and 600°C tempered materials, but in the 200°C tempered material were independent of strain rate. The relation between J_{IC} and $\dot{\varepsilon}$ can be expressed as follows:

$$J_{IC} = \alpha + \beta \, ln(\dot{\varepsilon}/\dot{\varepsilon}_0), \qquad \text{-----(4)}$$

where α and β are constants, and $\dot{\varepsilon}_0$ is the strain rate at the 0.1 mm/min crosshead speed, used to normalize the strain rate $\dot{\varepsilon}$. The values of α and β are presented in Table 3. It should be noted that the invariance of J_{IC} with strain rate in the 200 °C tempered material is similar to the invariance of the yield stress with strain rate, above.

Table 3 Values of constants α and β

Tempering temp. of specimens	α	β
200°C	3.14	0
400°C	8.41	-0.17
600°C	12.34	-0.27

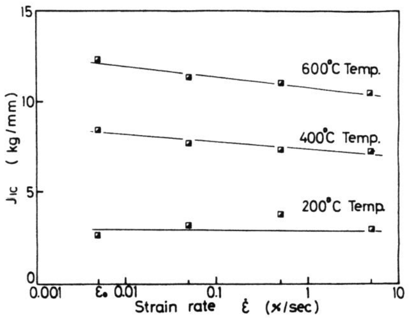

Fig. 8. Variation of critical J-integral value, J_{IC}, with $\dot{\varepsilon}$.

<u>Stretched zone width and fracture toughness</u>

The variation of the SZW at initiation with $\dot{\varepsilon}$ is shown in Fig. 9. The stretched zone width at initiation, s, is used to calculate J_{IC} and K_{IC} values from the following experimental equations, proposed by Nakamura (1976):

$$\left.\begin{aligned} J_{IC}(SZW) &= 86Es \\ K_{IC}(SZW) &= E\sqrt{86s/(1-\nu^2)}, \end{aligned}\right\} \text{----------(5)}$$

where E is Young's modulus (kg/mm^2) and ν is Poisson's ratio.

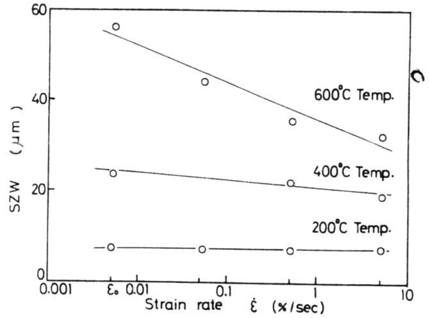

Fig. 9. Stretched zone width at initiation versus $\dot{\varepsilon}$.

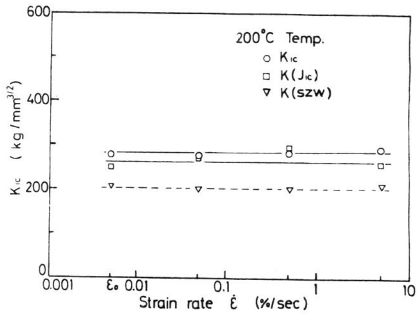

Fig. 10. Variation of differently derived values of K_{IC} with $\dot{\varepsilon}$ for the 200°C tempered material.

The values of K_{IC} as calculated from J_{IC} measured by the potential drop **method** , and from the stretched zone width, are shown in Fig. 10, Fig. 11 and Fig. 12 as a function of $\dot{\varepsilon}$. In addition, the values of K_{IC}, K_C and K_{max} obtained from ASTM E399 are also plotted, where K_C is the value of K_Q if K_Q is invalid, and K_{max} is the K value calculated from the maximum load.

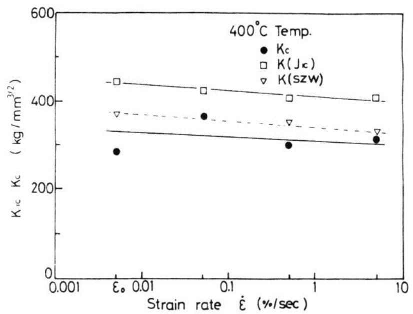

Fig. 11. Variation of differently derived values of K_{IC} with for the 400°C tempered material.

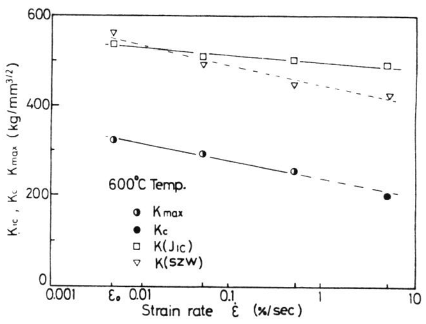

Fig. 12. Variation of differently derived values of K_{IC} with for the 600°C tempered material.

Low temperature fracture toughness

Fracture toughness tests were carried out from room temperature to -160°C. The resulting toughness values are plotted as a function of 1/T in Fig. 13. The open marks in this figure indicate valid K_{IC} values and the solid marks indicate invalid K_C or K_{max} values. All K_{IC} values for the 200°C tempered material in Fig. 13 fall on a straight line, implying an Arrhenius type equation.

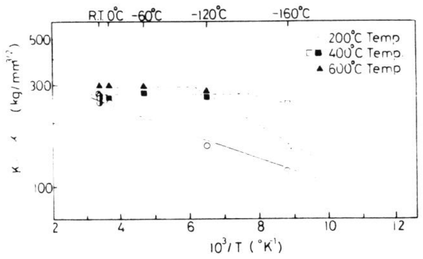

Fig. 13. Variation of fracture toughness with 1/T in the low temperature range.

DISCUSSION

K_{IC} values for the 200°C tempered material are greatly affected by temperature, but neither J_{IC}, K_{IC} nor the yield stress of the same material (Fig. 8 and Fig. 10) vary with strain rate. This indicates that changes in the yield stress can show directly the effect of strain rate on K_{IC} or J_{IC} values.

This can be seen in Fig. 14, where K_{IC} values calculated from the room temperature J_{IC} values obtained at four strain rates, together with low temperature K values at constant strain rate, are plotted against the yield stress measured under the same temperature and strain rate conditions.

Fig. 15 shows the toughness values in Fig. 14 replotted against the inverse temperature, 1/T, for the constant strain rate low temperature tests, or the inverse equivalent temperature for the room temperature variable strain rate tests, where the equivalent temperature is that temperature at which the yield stress as measured in the constant strain rate tensile tests is equal to the yield stress at room temperature at the given strain rate.

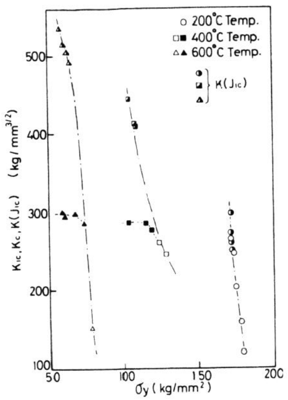

Fig. 14. Variation of fracture toughness with yield stress.
Open marks indicate valid K_{IC} values and solid marks invalid K_C or K_{max} values. Half-solid marks indicate K_{IC} values calculated from J_{IC}.

All K_{IC} values now fall on three straight lines, corresponding to the 200°C, 400°C and 600°C temtered materials respectively. That is, J_{IC} values at different strain rates which were obtained using a smaller specimen size than is permissible under ASTM E399 still obey the same Arrhenius equation as valid K_{IC} values measured at constant strain rate at low temperature, if the effect of the strain rate is normalized by using the equivalent temperature.

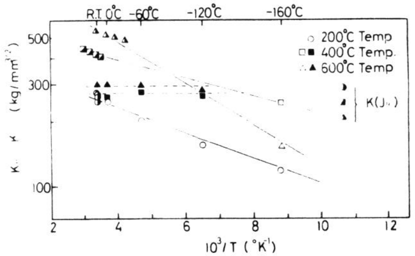

Fig. 15. Variation of fracture toughness with inverse temperature or inverse equivalent temperature, including K_{IC} values at four strain rates.
Symbols as for Fig. 14.

CONCLUSION

The following results were obtained:

(1) J_{IC} values were found to decrease with increasing strain rate, and could be expressed as follows:

$$J_{IC}=\alpha+\beta\, ln(\dot{\varepsilon}/\dot{\varepsilon}_0)$$

where, α, β:constants
$\dot{\varepsilon}$:strain rate
$\dot{\varepsilon}_0$:standard strain rate.

(2) J_{IC} values at high strain rates can be correlated with the fracture toughness at low temperature by means of the equivalent temperature, which can be derived from a comparison of the yield stress at various strain rates and the low temperature yield stresses measured at a constant strain rate.

ACKNOWLEDGEMENT

The authors wish to thank M. Aiba for the assistance of low temperature experiment, and also thank Kobe Steel Ltd for the provision of the material used in this study.

REFERENCES

Burns, S. J., and Z. J. Bilek (1973). Metallurgical Trans., 4, 975-984.
Corten, H. T. and A. K. Shoemaker (1967). Trans. ASME Ser. D, 89, 86-92.
Crosley, P. B., and E. J. Ripling (1969). Trans. ASME Ser. D, 91, 525-534.
Knott, J. F. (1973). Fundamentals of Fracture Mechanics, Butter worth, London.
Kraft, J. M., and A. M. Sullivan (1963). Trans. ASM, 56, 161

Merkle, J. G., and H. T. Corten (1974). Trans. ASME Ser. E, 96, 286-292.
Nakamura, H., H. Kobayashi, and H. Nakazawa (1976). Reprint of Japan Soc. Mech. Engrs., 760-13, 101-103.

Conversion into SI unit; $1 kg/mm^2 = 9.807 MN/m^2$; $1 kg/mm^{\frac{3}{2}} = 0.3101 MN/m^{\frac{3}{2}}$.